Journal of Colloid and Interface Science 461 (2016) 249–260

Contents lists available at ScienceDirect

Journal of Colloid and Interface Science

journal homepage: www.elsevier.com/locate/jcis

Tungstate sorption mechanisms on boehmite: Systematic uptake studies and X-ray absorption spectroscopy analysis

Hyuck Hur [a,1], Richard J. Reeder [b,*]

[a] Department of Chemistry, Stony Brook University, Stony Brook, NY 11794, USA
[b] Department of Geosciences, Stony Brook University, Stony Brook, NY 11794, USA

GRAPHICAL ABSTRACT

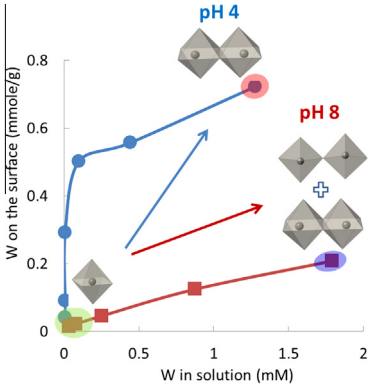

ARTICLE INFO

Article history:
Received 20 March 2015
Revised 1 September 2015
Accepted 2 September 2015
Available online 5 September 2015

Keywords:
Tungstate
Polytungstate
Isopolytungstate
Tungsten
Boehmite
AlOOH
Sorption
Polymerization
X-ray absorption spectroscopy

ABSTRACT

Mechanisms of tungstate sorption on the mineral boehmite (γ-AlOOH) were studied using batch uptake experiments and X-ray absorption spectroscopy. Batch uptake experiments over the pH range 4–8 and [W] = 50–2000 μM show typical oxyanion behavior, and isotherm experiments reveal continued uptake with increasing tungstate concentration without any clear uptake maximum. Desorption experiments showed that sorption is irreversible at pH 4 and partly reversible at pH 8. Tungsten L_1- and L_3-edge XANES spectroscopy indicates that all sorbed tungstates are octahedrally coordinated, even though the dominant solution species at pH 8 is a tetrahedral monotungstate. Tungsten L_3-edge EXAFS analysis shows that sorbed tungstate occurs as polymeric form(s), as indicated by the presence of corner- and edge-sharing of distorted tungstate octahedra. The occurrence of polymeric tungstate on the surface at pH 8 indicates that sorption is accompanied by polymerization and a coordination change from tetrahedral (in solution) to distorted octahedral (on the surface). The strong tendency for tungstate polymerization on boehmite can explain the continued uptake without an apparent maximum in sorption, and the limited desorption behavior. Our results provide the basis for a predictive model of tungstate uptake by boehmite, which can be important for understanding tungstate mobility, toxicity, and bioavailability.

1. Introduction

Until recently, little consideration has been given to the environmental impact of tungsten. This industrially important metal has been widely thought to be nontoxic in its pure or alloyed forms

* Corresponding author at: Department of Geosciences, Stony Brook University, Stony Brook, NY 11794-2100, USA.
E-mail address: rjreeder@stonybrook.edu (R.J. Reeder).
[1] Current address: Department of Earth and Environmental Sciences, Korea University, Seoul, Republic of Korea.

http://dx.doi.org/10.1016/j.jcis.2015.09.011
0021-9797/

[1,2]. Oxidation of metallic forms of tungsten results in dissolution and formation of soluble anions that are mobile in aquatic and soil systems under appropriate conditions of pH and redox potential [3]. The most stable oxidation state in surface environments is W (VI), tungstate, which forms many different oxyanions, including monooxyanion and polyoxyanion forms [4–6]. The study of tungstate behavior in the environment is complex due to the occurrence of multiple species associated with polymerization and their interactions with environmental materials. It is now recognized that the presence of dissolved tungstate may lead to adverse environmental effects, including soil acidification as well as toxic effects on plants, soil microorganisms and invertebrates [7–9]. Recent studies have shown that the toxicity of tungstate is related to its speciation. Strigul et al. studied toxicities of tungstate species in fish, and reported that polymeric tungstates were more toxic than monotungstate [10]. Investigation of tungstate behavior in aqueous systems, including its toxicity, has become increasingly important as industrial applications and releases to the environment have escalated.

Tungstate oxyanion speciation in solution depends on pH as well as total W concentration, showing some similarities with molybdenum oxyanion behavior [11,12]. Like molybdate, the dominant oxyanion species of tungstate at basic pH is monomeric WO_4^{2-} with tetrahedral coordination. As pH is decreased, tungstate forms polymeric species having mainly octahedral coordination as shown for selected species in Fig. 1 and described further in Supporting Information. Polymerization is favored with increasing tungstate concentration. In the VIB group, the tendency for polymerization increases with increasing atomic number, so that occurrence of polymeric forms of tungstate may be more common than molybdate for equivalent conditions [11]. Tungstate speciation has been studied by several researchers with ^{187}W nuclear magnetic resonance (NMR) spectroscopy, electrospray ionization mass spectrometry (ESI–MS), and Raman spectroscopy [4,5,13,14]. These studies have shown that general trends of tungsten polymerization are known under acidic conditions, yet the mechanisms are still not completely understood. Furthermore, the kinetics of formation of some polymeric species is sluggish, so that equilibrium speciation is not necessarily obtained over the time scale of laboratory experiments [4,5,11].

Sorption processes on mineral surfaces play an important role in regulating the distribution and mobility of trace metals in natural aquatic and soil systems. Tungstate has been shown to adsorb strongly on iron oxyhydroxide mineral surfaces at low pH conditions [15–17]. Hernandez performed sorption experiments and IR spectroscopy to characterize $H_2W_{12}O_{40}^{6-}$ sorption on iron and aluminum (hydr)oxide surfaces [15]. Gustafsson used a 2-p*K* Diffuse Layer Model and a 1-p*K* CD-MUSIC model to describe tungstate (and molybdate) sorption on ferrihydrite, accounting for monomeric and polymeric tungstates to fit the experimental data for both models [17]. The competitive sorption of tungstate and other oxyanions on goethite was studied by Xu et al. [16]. Tungstate sorption was found to be strongly competitive with molybdate and phosphate at the surface, whereas silicate and sulfate sorption were affected minimally by tungstate. Tungstate speciation in natural soils was studied by Clausen and Korte [2] and Bednar et al. [3], who found tungstate forming polymeric species with phosphate and silicate, and proposed a general transformation pathway for tungstates in nature. However, little is known of the influence that tungstate speciation plays in sorption behavior over a broader pH range and on other mineral sorbents. This fundamental information is important inasmuch as it may control tungstate mobility, toxicity, and bioavailability in natural systems.

In the present study, we investigate tungstate sorption behavior on the aluminum oxyhydroxide mineral boehmite, γ-AlOOH, over the tungsten concentration range 5–2000 μM. Although the lower end of this concentration range is more relevant environmentally, dissolved tungsten concentrations as high as 400 mg/L (2175 μM) have been reported at highly contaminated sites [2]. Boehmite occurs naturally as a common weathering product and is an effective sorbent for both cations and anions [18–21]. Tungsten L_1- and L_3-edge XANES spectroscopy was used to distinguish coordination environments around W atoms. The local structure and coordination of tungsten at the surface were determined using tungsten L_3-edge EXAFS, which allowed us to further characterize the binding mechanism as well as the dependence of tungstate sorption on environmental parameters such as pH, metal concentration, and ionic strength. This initial work provides a foundation for subsequent studies of tungstate sorption on other solids. The findings also have possible implications for tungsten toxicity in natural environments.

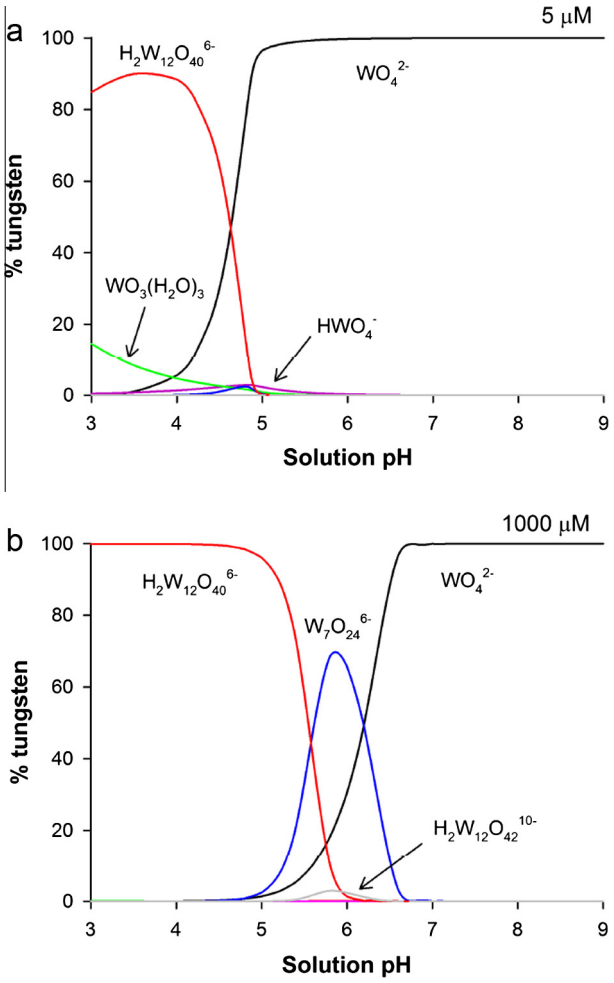

Fig. 1. Aqueous tungstate speciation at total tungstate concentrations of 5 and 1000 μM, calculated using the program PHREEQC with stability constants reported in Table S1 (Supporting Information) at ionic strength 0.01 M. Polymerization is favored with increasing tungstate concentration. Species present at low concentrations are not labeled.

2. Materials and methods

2.1. Sorbent

Boehmite from CONDEA Chemie GmbH was used in this study. Powder XRD was used to confirm the structure, and no other phases were detected. The specific surface area of the boehmite was found to be 136 m^2/g by five-point N_2 Brunauer–Emmett–Teller (BET) analysis. The point of zero charge (PZC) determined

for this material in previous studies lies in the range 8.6–9.1 [19,22].

2.2. Batch uptake experiments

Batch uptake experiments were conducted over a range of tungsten concentrations, from 50 to 2000 μM, at pH 4, 6, and 8. Ionic strength of 0.01 or 0.1 M was achieved using NaCl as a background electrolyte. Based on tungstate speciation calculations (see Supporting Information), pH 4 and 8 represent solution conditions for which polytungstates and monotungstate, respectively, represent the major components in the solution over the studied concentration range (Fig. 1). The pH 6 condition represents a mixture of monomeric and polymeric species, with proportions varying depending on total W concentration. The boehmite suspensions were equilibrated overnight before being titrated to the desired pH using HCl or NaOH. After an additional 24 h equilibration time, a pre-determined amount of a 0.1 M or 0.01 M Na_2WO_4 stock solution was added to 1 g/L boehmite suspensions to achieve the target W concentration. Small amounts of 0.1 M HCl or NaOH were used to adjust the pH after adding the Na_2WO_4 solution to the suspension. After 24 h of equilibration on a shaker table, the suspensions were centrifuged for 10 min at 10,000 rpm, and 10 mL aliquots of supernatant were collected from each sample. Tungsten concentration in the aliquots was measured with direct coupled plasma atomic emission spectroscopy (DCP-AES) to calculate the amount of tungsten sorbed on the boehmite surface. Selected samples were filtered using a vacuum pump, and the wet pastes were prepared for XAS analysis.

Tungstate stock solutions were prepared using $Na_2WO_4{\cdot}2H_2O$ (Alfa Aesar) and deionized water. The stock solutions were pre-titrated to target pH values prior to addition to the suspensions. To determine if pre-titration influenced sorption results, a set of parallel experiments was performed using freshly prepared stock solution without pre-titration. No discernible differences were found between results for these different stock solutions in terms of uptake or XAS.

All sorption experiments were performed under atmospheric conditions and no effort was made to purge CO_2 from the solutions. However, containers holding suspensions were kept sealed except for addition of stock solution and adjustments to pH, so CO_2 exchange was restricted. Nevertheless, the presence of dissolved CO_2 is expected to have some influence on the surface charge of boehmite in suspensions as a result of sorption. Su and Suarez examined the effect of carbonate sorption on surface charge of gibbsite ($Al(OH)_3$) and amorphous aluminum hydroxide, and showed that the observed PZC decreased by 0.5–0.7 pH units in suspension titrated with sodium carbonate solution [23].

2.3. Desorption experiments

Desorption experiments were conducted following the conclusion of sorption reactions (as described above) at two concentrations: 200 and 1000 μM. The final suspensions after 24 h reaction were centrifuged for 10 min at 10,000 rpm, the solution was discarded, and the moist particles were re-suspended in tungstate-free solution with the same pH condition and background electrolyte concentration. Aliquots (5 mL) were taken at designated time periods, and W concentration in the solution was measured by DCP-AES to allow calculation of sorbed W.

2.4. X-ray absorption spectroscopy

2.4.1. Tungsten L_1- and L_3-edge EXAFS and XANES

Tungsten L_1- and L_3-edge XANES and L_3-edge EXAFS data were collected at beamlines 20BM and 12BM at the Advanced Photon Source (APS, Argonne National Laboratory) and at X11A and X19A at the National Synchrotron Light Source (NSLS, Brookhaven National Laboratory). Spectra were collected at the W L_1 and L_3 edges using Si(1 1 1) monochromator crystals with detuning of 10–30%. Energy calibration was performed with a Ga filter (K-edge, 10.367 keV) or a W metal foil for the W L_3-edge (10.207 keV), and a Pt metal foil (L_3-edge, 11.564 keV) or a W metal foil for the W L_1-edge (12.2 keV). The monochromator was calibrated by assigning the indicated energy to the first peak of the derivative of the edge spectrum of the element used for calibration.

EXAFS and XANES spectra for model compounds were collected in transmission mode. Model compounds were mixed with boron nitride to achieve the proper edge step, and then loaded into Lucite sample holders and sealed using two layers of Kapton tape. All spectra for sorption samples and solutions were taken in fluorescence mode using a partially implanted planar silicon (PIPS) detector at the NSLS and a 13-element Ge detector at the APS. Wet pastes obtained from vacuum filtration of reacted suspensions were sealed in Lucite sample holders with Kapton tape and stored in sealed polyethylene bags with wet tissues to prevent drying. Samples were placed at a 45° angle to the incident beam for fluorescence measurements. Multiple spectra were routinely collected and averaged to achieve acceptable signal/noise.

2.4.2. Tungsten L_3-edge EXAFS fitting

Data analysis was conducted using the programs iFeffit [24] and WinXAS [25]. Shell by shell fitting was performed in real space using phases and amplitudes calculated by FEFF7 [26] based on published structures of selected reference compounds. Fitting strategies were developed and validated using EXAFS data collected from model compounds representing the wide variety of W(VI) coordination environments, including isolated tetrahedra and octahedra and various polymeric forms. Structures of these tungstate model compounds and EXAFS fit results are described in Supporting Information.

3. Results

3.1. Batch uptake trends

The effect of pH on tungstate sorption by boehmite was investigated at an initial tungstate concentration of 50 μM at two ionic strength conditions using NaCl as a background electrolyte (Fig. 2). Adsorption edges show the general behavior expected for anions, with maximum sorption in the pH range 5.0–5.5, and decreasing sorption with increasing pH, approaching minimum values near and above the PZC of boehmite, 8.6–9.1. A smaller decrease in sorption is observed at pH values below 5. The efficiency of W sorption is slightly affected by ionic strength. Slightly greater tungstate sorption is observed at 0.1 M NaCl for pH > 6, while the boehmite suspension at 0.01 M NaCl shows slightly greater sorption at pH < 5. The lower tungstate sorption with 0.1 M NaCl at pH < 5 might be explained by complexation with Na^+ in solution. The polymeric tungstate with large negative charge, e.g., $H_2W_{12}O_{40}^{6-}$, could form electrostatic bonds with Na^+ thereby reducing polytungstate sorption on boehmite at higher NaCl concentrations. The greater tungstate sorption at 0.1 M NaCl above pH 6 is similar to observations by Li et al. [27], who studied phosphate sorption on boehmite from the same source (CONDEA Chemie GmbH). These authors attributed greater phosphate uptake at higher NaCl concentration to Na^+ co-adsorption on the surface. However, it is possible that the greater sorption observed in 0.1 M NaCl suspensions at pH > 7 may reflect decreased competition with sorbed carbonate, which is expected to be less at the higher ionic strength [28,29]. At the lower ionic strength (0.01 M), greater carbonate

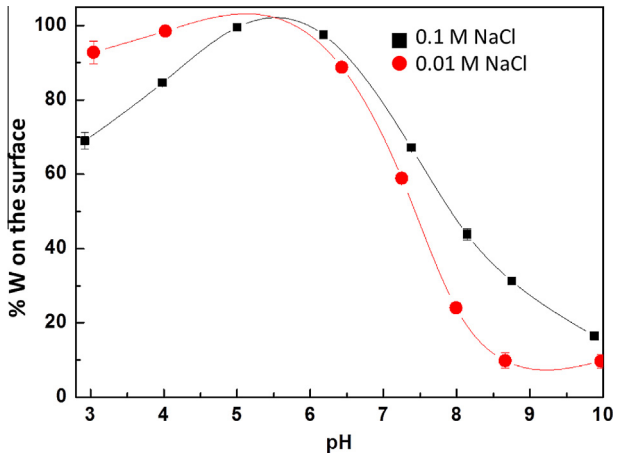

Fig. 2. Comparison of tungstate sorbed onto boehmite at different ionic strength conditions as a function of pH for 50 μM total tungstate.

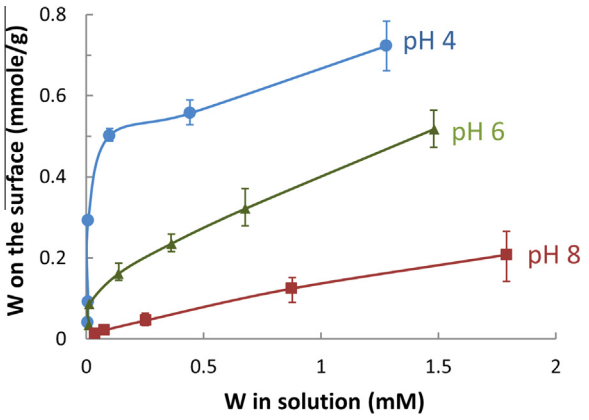

Fig. 3. Sorption isotherms of tungstate on boehmite as a function of pH at room temperature. No maximum in sorption is observed over the concentration range studied.

sorption would be more effective in shifting the PZC to lower values, so that less tungstate uptake would be expected.

Uptake experiments were performed to construct isotherms in the range 50–2000 μM total tungstate at pH 4, 6 and 8 (Fig. 3). These pH conditions were chosen to represent solutions in which polytungstate species (pH 4) or a monotungstate (pH 8) dominates, or in which a mixture is present (pH 6), as indicated by the speciation calculations described above. We performed initial kinetic experiments of tungstate sorption (initial [W] = 200 μM, and 0.19 mmol/g (0.84 W/nm^2) sorbed on boehmite at pH 4), which confirmed that sorption is fast, with ~80% of the equilibrium amount of tungstate sorbed within the initial few hours, and >90% sorbed within 24 h. On this basis, all subsequent sorption experiments were conducted over 24 h duration. In all pH conditions, the amount of W sorbed on the surface increased as W concentration in the solution increased, without reaching a maximum in the concentration range studied. As we expected from the pH edge experiments, W showed greatest sorption at pH 4. The tungstate surface coverage increased from 0.04 mmol/g to 0.72 mmol/g (0.18 to 3.19 W/nm^2) at pH 4, and increased from 0.01 to 0.21 mmol/g (0.04 to 0.93 W/nm^2) at pH 8.

3.2. Desorption experiments

Desorption experiments were performed at 200 and 1000 μM initial W concentrations at pH 4 and 8 to establish sorption reversibility. Tungstate sorbed for 24 h on boehmite at pH 4 showed largely irreversible behavior in desorption experiments, with more than 95% of the tungstate remaining on the surface for both initial concentrations studied. Sorption was found to be partly reversible at pH 8, as shown in Fig. 4. Approximately 25–30% of the tungstate on the surface was released into the solution at pH 8, with slightly greater release at 200 μM than at 1000 μM. These desorption results imply different sorption mechanisms on the boehmite surface at pH 4 and pH 8. X-ray absorption spectroscopy was used to provide further insight into dominant sorption mechanisms.

3.3. Tungsten L_1- and L_3-edge XANES

3.3.1. W L_1-edge XANES

Both the L_1- and L_3-edge XANES spectra of tungsten have proven useful for characterizing tungstate coordination environments [30]. A pre-edge feature is observed in the L_1 edge, associated with electron transitions from 2s to unoccupied valence orbitals. This transition is dipole forbidden in symmetric octahedral environments, but allowed for tetrahedral and distorted octahedral environments. Previous studies have shown that the intensity and shape of the pre-edge feature relate to coordination and degree of (octahedral) distortion [31]. Reference compounds that contain only tetrahedrally coordinated W(VI), which include $Na_2WO_4{\cdot}2H_2O$ and $CaWO_4$, exhibit a prominent high-intensity peak in the pre-edge region (Fig. S3 in Supporting Information). In contrast, reference compounds with only octahedral coordination, such as Ba_2NiWO_6, TBA-W_6O_{19}, phosphotungstic acid, and WO_3, display pre-edge peaks that are lower in intensity and different in shape than tetrahedral compounds. Furthermore, because the intensity of the pre-edge feature for octahedrally coordinated compounds is sensitive to the degree of distortion, differences in pre-edge intensity and shape are evident among the various octahedral compounds (see Section 4 in Supporting Information for further description). The pre-edge features for all the sorption samples are found to be similar to one another, with pre-edge intensities lower than those in tetrahedral reference compounds, and most closely matching reference samples with distorted octahedral coordination, such as phosphotungstic acid.

3.3.2. W L_3-edge XANES

Tungsten L_3-edge XANES has been studied less than the L_1-edge. Recently, Yamazoe et al. demonstrated that second derivatives of the L_3-edge show differences corresponding to coordination environment, analogous to the ligand field splitting of 5d orbitals observed for different coordination environments of Mo(VI) [30]. Second derivative L_3-edge XANES spectra of reference samples containing only W(VI) tetrahedra show a single minimum with a weak shoulder on the low-energy side, as observed for $Na_2WO_4{\cdot}2H_2O$ and $CaWO_4$ (Fig. 5). Model compounds containing only W(VI) octahedra show splitting in the second derivatives to create two minima. Yamazoe showed that the shape of the minima and the degree of splitting between them are dependent on the coordination type and the degree of distortion of the octahedra [30]. Fig. 5 also shows second derivatives of W L_3-edge XANES spectra of the lowest W concentration sorption samples (5 μM) at pH 4 and 8, compared with tetrahedral and octahedral model compounds. Findings for higher concentration sorption samples are summarized in Supporting Information (Table S2). Second derivative spectra of both sorption samples display two well separated minima, consistent with distorted octahedral coordination of W(VI). Notably, these second derivative spectra are nearly identical for samples at both pH conditions. In Fig. 5, sorption samples are clearly distinguished from $Na_2W_2O_7$, which contains both tetrahedral and octahedral W(VI). Although it is not possible to rule out a

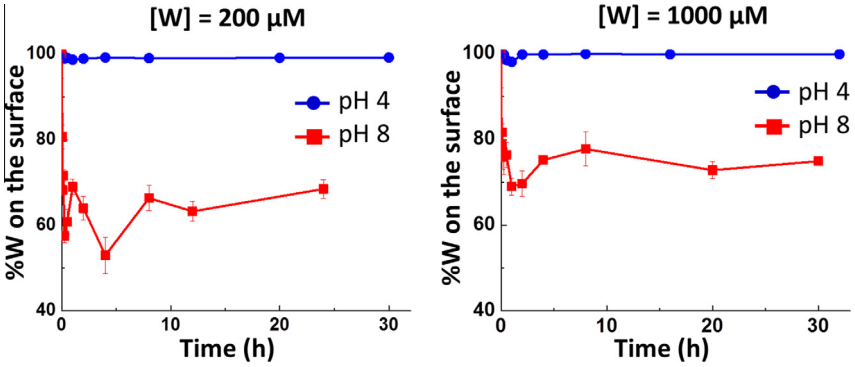

Fig. 4. Tungstate desorption from boehmite at pH 4 (squares) and 8 (circles) as a function of time, at 200 and 1000 µM total tungstate.

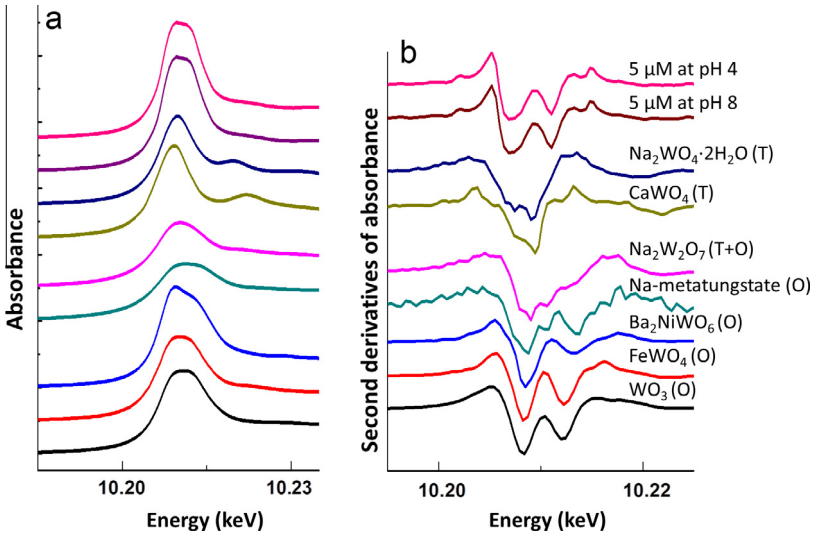

Fig. 5. Tungsten L_3-edge XANES spectra (a) and corresponding second derivative spectra (b) for selected model compounds showing differences that distinguish tetrahedral (T) and octahedral (O) coordination of W(VI). Spectra for 5 µM sorption samples are shown at top for pH 4 and 8.

minor contribution from tetrahedrally coordinated W(VI), the dominant component in the sorption samples is clearly octahedral, and the octahedra are distorted on average.

3.3.3. Combined L_1-edge and L_3-edge XANES

By combining the pre-edge peak area from L_1-edge XANES with the energy separation between minima in the L_3-edge second derivatives, clear differences are evident among W(VI) coordination environments (Fig. 6). $Na_2WO_4{\cdot}2H_2O$ and $CaWO_4$, both with tetrahedrally coordinated W, lie at one end of a trend, distinguished by a large pre-edge area in W L_1-edge XANES and a small energy separation in W L_3-edge second derivatives. On the other end of this trend lies Ba_2NiWO_6, with perfect octahedral coordination, having a relatively small pre-edge area and a large energy separation in the second derivative minima. Reference compounds with more distorted octahedra, such as WO_3, phosphotungstic acid, and sodium metatungstate, lie at intermediate positions along the trend, reflecting intermediate values of pre-edge peak area and energy separation. All of the sorption samples are tightly clustered at an intermediate position along the trend (within the yellow circle, Fig. 6). Their proximity near $Na_2W_2O_7$, which contains both tetrahedral and octahedral W(VI), might suggest that the sorption samples also contain mixtures of W(VI) tetrahedra and octahedra. However, the second derivative spectra for the L_3-edge (Fig. 5) clearly indicate that all sorption samples have octahedrally coordinated W(VI), as described in the previous section.

3.4. W L_3-edge EXAFS

3.4.1. Model compounds and tungstate reference solutions

W L_3-edge EXAFS provides further insight to local structure of sorbed W(VI). Fitting of selected reference compounds and aqueous tungstate solutions demonstrated that it is possible to distinguish polymeric and monomeric species, and allowed us to formulate a fitting strategy for sorption samples. EXAFS chi functions and corresponding Fourier transforms are shown in Fig. 7 for selected model compounds and aqueous tungstate solutions at pH 4 and 8. Fitting results are summarized in Supporting Information Table S3.

The 1 mM pH 4 and 8 solutions show distinct differences in their chi curves and FT magnitudes (Fig. 7). The chi function for the pH 8 solution shows a single beat, and the FT magnitude shows a corresponding single peak, similar in character to the $Na_2WO_4{\cdot}2H_2O$ reference sample, which contains only tungstate tetrahedra. The pH 8 solution data were best fit with a single shell of W–O atoms at 1.78 Å, which is characteristic of tetrahedral W(VI) coordination, and consistent with the dominance of monomeric tetrahedral species expected at pH 8 and confirmed by electrospray ionization mass spectroscopy (ESI–MS) (see Supporting Information). In contrast, the pH 4 solution shows several oscillations with different

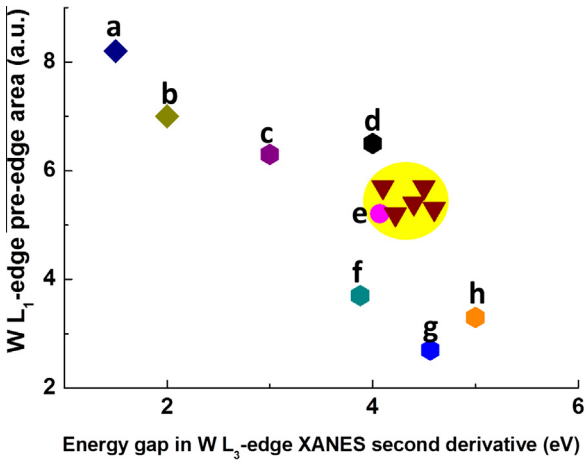

Fig. 6. Relationship between the splitting of the minima in the L_3-edge XANES second derivatives and the pre-edge peak area (a.u.) of L_1-edge XANES. (a) $Na_2WO_4{\cdot}2H_2O$, (b) $CaWO_4$, (c) phosphotungstic acid, (d) WO_3, (e) $Na_2W_2O_7$, (f) sodium metatungstate, (g) Ba_2NiWO_6, (h) TBA-W_6O_{19}. All sorption samples are tightly clustered (yellow circle). Sorption samples are summarized in Supporting Information (Table S2). (For interpretation of the references to color in this figure legend, the reader is referred to the web version of this article.)

phases in the chi curve, with evident splitting in the first two oscillations, similar to the splitting observed for the polymeric reference samples (Fig. 7). The FT magnitude for the pH 4 solution shows a split first peak with weaker peaks at higher *R*. The split first peak compares with the polymeric reference compounds but with a different asymmetry in intensities. The distinguishing feature of polytungstates is connected W(VI) octahedra, which should be evident in FT data as peaks at greater distances, like those seen in model compounds (Fig. 7). The peaks in the range 3.3–3.8 Å are consistent with edge- and corner-sharing of tungstate octahedra, and confirmed by fitting reference compounds. At pH 4, polymerization is favored, with $H_2W_{12}O_{40}^{6-}$ being the dominant aqueous species based on the calculations (Fig. 1; see Supporting Information) and confirmed by the ESI–MS results (Fig. S2 in Supporting Information) showing the likely presence of multiple polytungstate species. The structure of $H_2W_{12}O_{40}^{6-}$ contains two distinct W–W distances, ~3.3 Å for edge-sharing and ~3.8 Å for corner-sharing. These distances are consistent with our EXAFS result for the solution at pH 4. However, it is not possible to uniquely identify the metatungstate species or to rule out the presence of other polymeric tungstate species, inasmuch as they share the distinctive edge- and corner-sharing of W(VI) octahedra, and would not be distinguishable by EXAFS. Nevertheless, the EXAFS results confirm the dominance of polymeric tungstate species in the pH 4 solution, whereas the pH 8 solution contains monomeric tetrahedral tungstate.

3.4.2. Tungstate sorption samples

The W L_3-edge EXAFS of tungstate-sorbed boehmite samples at different tungstate concentrations and pH conditions are compared in Fig. 8. Based on the experimental isotherms, we chose sorption samples for EXAFS study at three total W concentrations: 5, 200, and 1000 μM. At pH 4, these concentrations result in coverages of 0.022, 0.197, and 0.557 mmol/g (or 0.10, 0.87, and 2.47 W/nm^2). The surface coverages at pH 8 are 0.007, 0.014, and 0.125 mmol/g (0.03, 0.06, and 0.55 W/nm^2). The most striking observation is that the chi functions are broadly similar for all samples, yet small, distinguishing differences are evident (Fig. 8). All chi functions show a split first oscillation and a sharp second oscillation apparently from interference with a second or additional beat. The 200 and 1000 μM pH 4 samples exhibit an asymmetry in the split first oscillation in the chi function compared to other samples, as well as a different or additional phase obvious at higher *k* values.

The corresponding FT magnitudes show generally similar first peaks, corresponding to first-shell W–O coordination, but important differences are evident in weaker peaks at higher *R* values. For the lowest concentration samples, 5 μM tungstate, no discernible differences are evident between pH 4 and 8 conditions. We note that FT magnitudes for the 200 and 1000 μM pH 8 sorption samples are nearly identical to one another, exhibiting peaks in the range 3.0–3.5 Å (Fig. 8, not corrected for phase shifts), which are consistent with backscattering from W or Al. These pH 8 samples are distinct from the same concentration samples at pH 4, which show different peaks in the range 3.0–3.5 Å. The 5 μM samples are different from the higher concentration samples at both pH 4 and pH 8, as indicated by the absence of distinct peaks at

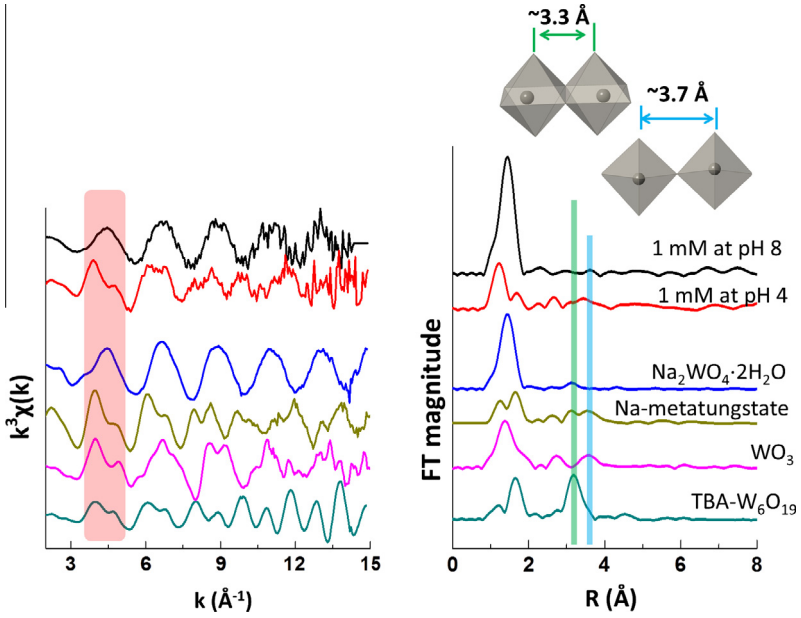

Fig. 7. Tungsten L_3-edge EXAFS chi functions (left) and corresponding Fourier transform magnitudes (right, not corrected for phase shifts) for 1 mM tungstate solutions (pH 4 and 8) and selected model compounds. Schematic representations show typical W–W distances associated with edge- and corner-sharing of tungstate octahedra.

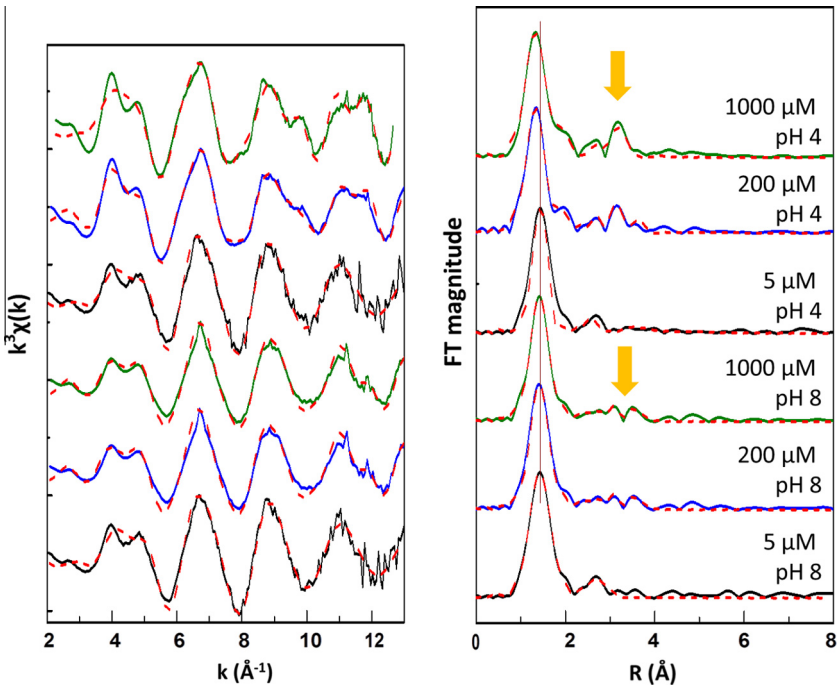

Fig. 8. Tungsten L_3-edge EXAFS chi functions (left) and Fourier transform magnitudes (right) for tungstate sorbed on boehmite. Solid lines are data and dashed lines are fits. Arrows indicate the primary differences between high concentration pH 4 and pH 8 sorption samples.

3.0–3.5 Å. Fitting described in the following section provides further insight about local structure.

3.5. W L_3-edge EXAFS fitting

The primary challenges in fitting W L_3-edge EXAFS spectra for sorption samples arise from the existence of multiple, overlapping paths for polymeric species and the likely existence of multiple species, particularly at high tungsten concentrations. A distinction between tetrahedral and octahedral coordination can be made on the basis of average, first-shell W–O distances. The average W–O distance in tetrahedral tungstates is ~1.8 Å, whereas polytungstates have longer average W–O distances (~1.95 Å), reflecting their octahedral coordination. However, the octahedral coordination in polytungstates is invariably distorted, resulting in a range of individual W–O distances (1.76–2.4 Å). Because of the distortion observed in W octahedra, fitting typically required two or more W–O paths, whereas tetrahedral W was best fit with a single W–O path. Although the common polymeric tungstate species differ in the details of their configuration, they share several common characteristics that distinguish them from monomeric, tetrahedral species. Tungstate octahedra may be connected by corner- and/or edge-sharing, and the corresponding W–W distances can generally be distinguished. Although some overlap exists for the range of characteristic distances for edge- vs. corner-sharing, peaks in the range 3.3–3.8 Å that are fit well by W–W paths provide clear evidence of polymeric tungstates, even if the exact species cannot be identified. Further complications in fitting may result if multiple polymeric species exist.

The general fitting procedure followed three steps. First, the main peak corresponding to first-shell W–O backscattering was fit using one or more paths. The best fits for sorption samples were typically achieved using two or three W–O paths for the first main peak in FT magnitude. Second, a near-linear O–W–O multiple scattering (MS) path was introduced. Multiple scattering is found to have an effect mainly at low k in the chi functions, and accounting for it was found to be necessary to achieve acceptable agreement with the observed splitting in the first oscillation near 3.5–5 $Å^{-1}$. Finally, the peaks in the range 3.0–3.8 Å were fit with W–W and/or W–Al paths. Reference compounds were fit to validate the strategy described, however, their coordination numbers were constrained to be consistent with known structure data.

The EXAFS data for the lowest concentration sorption samples were fit first with single scattering paths for octahedral coordination. We constrained total coordination number of the first shell to 6 if the fit results were not reasonable with floating coordination numbers. We assumed that a W–Al path contributes to the EXAFS signal for all sorption samples, so the parameters of a W–Al path, obtained from the fit results of the 5 µM sorption sample, were fixed in the fitting process. The fit results of higher concentration samples were compared with and without a W–Al path adopted from the result of the lowest concentration sample. We also included up to two W–W paths, corner- and edge-sharing, to fit the second shell for the higher concentration samples.

Fit results for all sorption samples are summarized in Table 1, and fits for representative samples are shown in Fig. 8. Both 5 µM tungstate sorption samples (pH 4 and 8) were fit best with two W–O paths (1.75 and 2.14 Å) for the first peak with a combined coordination number (CN) of 6.3 (±1.2). This gave a clearly better fit than a single path. The split first shell, with an average W–O distance of 1.95 Å, is consistent with octahedral coordination in which the W atom is off-centered, confirming that the dominant W(VI) component sorbed on boehmite is octahedrally coordinated. This finding agrees with W L_1- and L_3-edge XANES results, showing distorted octahedral coordination for both pH 4 and 8 sorption samples. Based on fits of polymeric tungstate model compounds (Supporting Information), and consistent with the findings of Kuzmin et al. [32], it was necessary to introduce a multiple scattering contribution to satisfactorily fit the splitting in the first oscillation in the chi functions at 3–3.5 $Å^{-1}$. A four-leg, near linear O–W–O path, based on the configuration in sodium metatungstate, was found to be most suitable. The weak peak at 2.7 Å in the FT (not corrected for phase shift) was alternately fit with a W–Al path and a W–W path. The fit with 2.2 Al at 3.14 Å was favored,

Table 1
Summary of EXAFS fitting results for tungstate-sorbed boehmite samples.

Sample	Path	CN[a]	R (Å)[b]	σ^2 (Å^2)[c]	ΔE_0 (eV)
5 μM pH 4 and 8	W–O1	3.1	1.75	0.002	3.4
	W–O2	3.2	2.14	0.009	
	W–Al	2.2	3.14	0.01	
1000 μM pH 8	W–O1	3.0	1.75	0.003	−0.4
	W–O2	4.0	2.14	0.009	
	W–Al	2*	3.14	0.012	
	W–W1	0.6	3.23	0.004	
	W–W2	1.6	3.73	0.007	
200 μM pH 4	W–O1	2*	1.73	0.003	−4.1
	W–O2	2*	1.90	0.019	
	W–O3	2*	2.19	0.007	
	W–Al	2*	3.19	0.012	
	W–W	2.4	3.25	0.008	
	W–W	1.3	3.69	0.008	
1000 μM pH 4	W–O1	2*	1.74	0.003	−1.2
	W–O2	2*	1.98	0.019	
	W–O3	2*	2.21	0.006	
	W–Al	2*	3.15	0.015	
	W–W	3.4	3.25	0.008	

* Fixed in the fitting.
[a] Coordination number (±20%).
[b] Distance in Å (±0.02 Å).
[c] Debye–Waller factor.

inasmuch as fits with a W–W path gave a distance (2.8 Å) considered to be unrealistically short. Furthermore, the intensity of this peak decreases as tungstate concentration increases in the solution.

Fitting of the 200 and 1000 μM pH 8 samples gave nearly identical fit results. The first peak was again best fit with two W–O paths at 1.75 and 2.14 Å. A MS path was again found to be necessary, and a W–Al path was fit at 3.14 Å. The peaks near 3.3–3.8 Å were best fit with two W–W paths at 3.23 and 3.73 Å, with combined CN of 2.2 ± 0.4. Fits for these peaks were also attempted with W–Al paths, however, these fits were either not satisfactory or resulted in W–Al distances that were not reasonable. The peaks near 3.3–3.8 Å appear with increasing tungstate concentration, while the peak at 3.1 Å in the 5 μM pH 8 sample diminishes as tungstate concentration increases, indicating that increasing W–W coordination (near 3.3–3.8 Å) is linked to tungstate concentration.

The 200 μM sorption sample at pH 4 was best fit with three W–O paths at 1.73, 1.90 and 2.19 Å, and a W–W path at 3.25 Å. In fitting the 200 μM sorption sample, a second W–W path was introduced to fit the right shoulder near 3.3 Å in the FT (not corrected for phase shift), which is similar to the feature in the sorption samples at pH 8. The 1000 μM sorption sample was best fit with three W–O paths at 1.74, 1.98, and 2.21 Å. The coordination number for the first shell of the 200 μM and 1000 μM samples at pH 4 was set to a value of 6 based the W L_1- and L_3-edge XANES results. We constrained the CN of each W–O path to 2 based on the W–O paths in model compounds. Fits using two and three W–O paths constrained to total CN of 6 were compared for fitting the first peak in the FT. Not surprisingly, the use of three W–O paths gave a better fit to the first oscillation in the chi function and the first peak in the FT, but neither case fit the observed splitting of this oscillation ideally. Fit results were compared with and without a W–Al path, with slightly better results obtained by including W–Al, and especially the small feature near 2.5 Å in the FT (not corrected for phase shift) occurring at the same position of the W–Al path in the 5 μM sorption samples. The second shell in the 1000 μM pH 4 sample was best fit with a W–W path near 3.25 Å, consistent with edge-sharing W–W. This peak also increases with increasing tungstate concentration in the solution. We also attempted fits using additional W–W paths to explore possible destructive interference resulting from multiple closely spaced W–W backscattering paths. However, this resulted in unrealistic parameters with no clear improvement in fit results. The main difference between the higher concentration pH 4 and pH 8 spectra appears to be a greater degree of W–W edge-sharing in the pH 4 spectra compared to the pH 8 samples, suggesting some differences in the respective polymeric sorption complexes.

4. Discussion

4.1. Tungstate sorption trends on the boehmite surface

Tungstate shows a strong affinity for sorbing onto boehmite at low and neutral pH conditions, with decreasing uptake at higher pH. Observed uptake near or above the PZC value of boehmite (pH 8.6–9.1) suggests that tungstate sorption is not due entirely to electrostatic attraction. This result is consistent with previous studies investigating the reaction of tungstates with other mineral surfaces [16,17,33]. The absence of a maximum in uptake of tungstate with increasing concentration in the solution suggests that tungstate sorption on the surface is not limited by the surface site availability over the range studied. We note that a study of the sorption of the $H_2W_{12}O_{40}^{6-}$ polymeric species on boehmite at initial pH 5 observed a sorption maximum reported as 0.08 μmol $H_2W_{12}O_{40}^{6-}$ per m^2 (equivalent to 0.6 W/nm^2) at $H_2W_{12}O_{40}^{6-}$ solution concentrations above ~100 μM (or 1200 μM W(VI)) [15]. Direct comparison with our results is complicated by the different experimental conditions used. Their solution pH (initially 5) was allowed to drift during uptake, increasing rapidly to pH 7 and decreasing to ~6.3 at 48 h. They presented spectroscopic evidence suggesting that the $H_2W_{12}O_{40}^{6-}$ polymeric species remains largely intact on sorption. As described below, we are unable to confirm the identity of sorption complexes and consider that multiple species may be present. Nevertheless, it is interesting to compare observed sorption densities with the prior study. For example, the surface coverages from our 1000 μM sorption experiments at pH 6 and 8 (which bracket the final pH in [15]) are 1.42 and 0.55 W/nm^2, respectively. These values are not greatly different than the coverage observed in the prior study (0.6 W/nm^2) [15].

The desorption experiments show that tungstate uptake is essentially irreversible at pH 4 and only partly reversible at pH 8. Sorption irreversibility is commonly attributed to formation of a surface precipitate or a stable surface complex, where release of the adsorbate to solution is restricted either because of its greater stability on the solid or due to a kinetic hindrance [34,35]. Our desorption results imply some differences in sorption complexes on the boehmite surface at pH 4 and pH 8.

4.2. Tungstate polymerization and coordination change on the boehmite surface

The most striking finding in our study is the occurrence of polymeric tungstates at the boehmite surface from sorption experiments at both pH 4 and 8, except possibly for the lowest tungstate concentration (5 μM). While not surprising for pH 4 sorption samples, this finding was unexpected at pH 8, where monotungstate dominates in solution. Whereas the XANES signatures of the sorbed polymeric tungstates are almost indistinguishable between these two pH conditions, the EXAFS results show small but distinct differences between pH 4 and 8. The L_1- and L_3-edge XANES results confirm distorted octahedral coordination of W(VI) for all sorption samples (Figs. 5 and 6). The L_3-edge EXAFS fits are consistent with such coordination, and also confirm W–W distances that correspond directly to corner- and edge-sharing of

W(VI) octahedra, except for the 5 μM sorption samples. These XANES and EXAFS signatures are distinguishing characteristics of polymeric tungstate species. However, because many different polytungstates share these features in various combinations, there is little likelihood of identifying individual species. It is also possible, perhaps even likely, that multiple tungstate species occur on the boehmite surface. Possible supporting evidence may be found in the change of EXAFS results with increasing concentration. ESI–MS results show several types of polytungstates in pH 4 solution, and previous studies have reported various intermediate polytungstate species [4,5,13]. Those polymeric tungstates are possible candidates for surface complexes. Yet, the XANES and EXAFS of the sorption samples do not match exactly any particular model compounds that we examined. While the ESI–MS results for the pH 4 solution show monotungstate and several polytungstates, monotungstate is the dominant species in solution at pH 8 (Supporting Information). Our XANES and EXAFS results confirm polytungstates as the major surface complexes. However, it is not possible to entirely rule out the occurrence of a minor component of tetrahedral tungstate co-existing with polymeric forms on the surface, owing to limited sensitivity of the method.

The occurrence of one or more polymeric tungstate species in the higher concentration sorption samples at pH 4, where polymerization dominates in solution, is not surprising. However, our results for the 200 and 1000 μM samples at pH 8 lead us to conclude that one or more polymeric tungstate species forms during uptake at the boehmite surface, inasmuch as the dominant solution species is a monomer. Furthermore, this is accompanied by a change from tetrahedral coordination of W(VI) in solution to octahedral coordination in the polymeric surface complex, a change that also occurs with the 5 μM samples. The precise details of how the polymerization and change in coordination occur remain unclear, as does the actual form of the surface species. Yet, interaction of tungstate with the boehmite surface seemingly favors a coordination change and polymerization. Previous studies of tungstate sorption on iron and manganese oxides have suggested the existence of monomeric tungstate with octahedral coordination on the surface at pH 8 [33]. However, the tungstate concentrations used in that study (0.15–100 μM) were restricted to the lower end of the range in our study (5–1000 μM), so that only our lowest concentration sample can be compared with their results. Our results are consistent with octahedral coordination of W(VI), and the absence of clear W–W backscattering provides plausible evidence for a monomeric tungstate on the surface at this low W concentration (5 μM). However, we cannot entirely rule out the possibility that polymeric tungstate exists on the surface, especially at pH 4 where the polymeric species $H_2W_{12}O_{40}^{6-}$ is dominant in solution. We also note that Clausen et al. reported polytungstate species present in firing range soils at pH 6, with EXAFS data suggesting an α-Keggin type cluster [36]. We are not aware of any reports of polymeric tungstate sorption complexes at basic pH conditions.

4.3. Identification of tungstate species at the surface

The inability to identify the particular species of sorbed polymeric tungstate(s) because of the similarities they share in coordination and configuration raises interesting questions. First, do multiple species occur at the surface, i.e., more than one type of polymeric unit? This possibility might be anticipated at low pH because of the presence of multiple polytungstate species in solution, some of which may be metastable species associated with slow polymerization kinetics. The subtle changes observed in EXAFS with increasing W concentration at pH 4 may reflect the appearance of additional surface species at the higher end of the concentration range (Fig. 8), or possibly related to sorption exceeding available surface sites. Active adsorption site densities on boehmite have been reported for PO_4^{3-} (0.79/nm^2) [19] and $H_2W_{12}O_{40}^{6-}$ (0.05/nm^2) [15]. The latter site density corresponds to 0.6 W/nm^2. In comparison, the surface coverage for our 5 μM sorption sample at pH 4 is 0.10 W/nm^2, and those for the 200 and 1000 μM samples are 0.87, and 2.47 W/nm^2, respectively. These latter surface coverages likely exceed available adsorption sites.

A related question is whether the differences in sorption reversibility between pH 4 and 8 can be explained by different surface complexes. Sorption at pH 4 is largely irreversible, whereas at pH 8 some reversibility (25–30%) is observed (Fig. 4). The EXAFS results reveal differences in the W–W paths between pH 4 and pH 8 samples (for both 200 and 1000 μM), suggesting structural differences in the surface complexes, which could be responsible for the differing desorption behaviors. The presence of multiple surface species at one of the pH conditions could also influence the observed behavior. The pH may also play some role in controlling the observed sorption reversibility, as suggested by polymerization behavior in solution. At low pH polymerization of W(VI) is clearly favored, whereas at near neutral and higher pH monomeric tungstate is favored. Hence, one could speculate that the polymeric surface complexes are more stable at pH 4 than at pH 8. This would be consistent with irreversible sorption at the lower pH but with some limited degree of reversibility at the higher pH. The effect of pH on surface charge may also play a role in sorption reversibility. The more positively charged surface at pH 4 would create more favorable circumstances for sorbed polytungstates, which have large negative charges.

It is interesting to consider whether formation of polymeric tungstates at the surface is analogous to surface precipitation. In both cases, W(VI) forms extended structures at the surface. We consider that no distinction between them would be possible using EXAFS.

4.4. Comparison with molybdate sorption on (hydr)oxide surfaces

In view of the similarities noted between tungstate and molybdate systems, it is interesting to compare their sorption behavior. Molybdate shows a distribution of species in solution broadly similar to tungstate, favoring monomeric species at neutral and high pH and formation of polymeric species at low pH [11]. Arai investigated molybdate species sorbed on the goethite (FeOOH) surface using Mo K-edge EXAFS [37]. This study reported the existence of monomeric tetrahedral molybdate at the surface at near neutral pH and a mixture of monomeric tetrahedral and polymeric octahedral molybdate at acidic pH. Increasing Mo loading favored the formation of the polymeric form. Wasylenki et al. used Mo K-edge EXAFS to investigate molybdate species sorbed on birnessite (MnO_2) [38]. In sorption experiments performed at pH 8.0–8.5, where monomeric tetrahedral molybdate is the dominant solution species, they found the sorbed species to be a polymeric molybdate with distorted octahedral coordination. This finding differs from the results of Arai at near neutral pH, where monomeric tetrahedral molybdate was reported. This difference may reflect the differing properties of the sorbent phases and/or their surface charge. However, both studies identified the tendency for molybdate to polymerize when sorbed at metal (hydr)oxide surface, although at different pH conditions. In our study, we find that tungstate exhibits a strong tendency to form a polymeric species on the surface of boehmite over a wide range of pH and tungstate concentrations. Only at the lowest concentration (5 μM), do we find evidence for a monomeric octahedral complex. At pH 8, sorption is accompanied by a change in W(VI) coordination from tetrahedral (in solution) to distorted octahedral (on the surface). The tendency that we observe for polymerization of tungstate over the entire pH range 4–8 may reflect the different sorbent (boehmite) and/or a

greater inherent tendency for tungstate to polymerize compared to molybdate. Further studies of tungstate sorption on different mineral surfaces are needed to evaluate the importance of surface-driven tungstate polymerization.

4.5. Possible mechanisms for tungstate polymerization and coordination change on the boehmite surface

The coordination change and the polymerization of tungstate sorbed on boehmite at pH 8 were observed by XANES and EXAFS in our study. However, the mechanisms still remain unclear. We speculate that formation of an inner-sphere surface complex could induce the observed symmetry change from tetrahedral WO_4^{2-} to octahedral coordination, with the addition of water molecules. Like other tetrahedral oxyanions (e.g., PO_4^{3-}), we presume that tetrahedral tungstate would initially form a bidentate binuclear surface complex on the boehmite surface at pH 8 [27]. Our EXAFS fit results for the 5 μM sorption sample at pH 8 support formation of an inner-sphere, octahedral complex, showing a W–Al path at 3.14 Å. The W–O bonds for the oxygen atoms bridging with Al atoms at the surface would lengthen, thereby lowering their bond strengths and also allowing introduction of water molecules that ultimately result in the change to octahedral coordination (Fig. S4). Previous XANES and EXAFS studies of tungstate species deposited on prepared Al_2O_3 surfaces observed the coordination change of tetrahedral tungstate to octahedral dependent on the availability of water molecules at the surface [39,40]. This model suggests that the sorption mode(s) of tungstate on the surfaces plays an important role in the coordination change.

Similar results were observed in previous studies of molybdate species on various oxide catalyst surfaces, such as δ-MnO_2, TiO_2, ferrihydrite, Al_2O_3, goethite, and hematite [41–46]. In these studies, molybdates forming inner-sphere complexes on δ-MnO_2, TiO_2, and hematite were found to have octahedral symmetry, while tetrahedral molybdates found on ferrihydrite and Al_2O_3 surfaces were interpreted to form outer-sphere complexes [47]. The different coordination geometries of Mo on Fe (oxyhydr)oxides imply that specific properties of the surface influence the coordination change and that the coordination change was induced by the inner-sphere surface complexation of Mo in these studies. Further studies of tungstate sorption on various mineral and oxide surfaces are needed to reveal whether similar relationships exist between the properties of the mineral surface and the coordination of adsorbed tungstate species.

We can envision two possible surface polymerization mechanisms to explain our observations at pH 8: (1) the polymerization of neighboring tungstate species sorbed on the surface and (2) additive polymerization with a tetrahedral complex in a terminal position. Schematic models for these mechanisms are shown in Fig. 9. The former should be dependent on a sufficiently high surface coverage of tungstate to allow linkages that result in edge- or corner-sharing of tungstate octahedra. We note that this mechanism may not be consistent with the continued tungstate uptake that we observed in the isotherm results, since this model requires that polymerization occurs only between tungstate groups sorbed on the surface.

The second model is an example of open-chain polymerization and is similar to the tungstate polymerization mechanism suggested by Walanda et al. in solution based on ESI–MS results [13]. Monotungstate surface complexes, which would be octahedral as described above, could act as preferred sites for attachment of tetrahedral tungstate species in solution. Hence, the terminal tetrahedral tungstate is available to form tungstate chains with additional monomers. Additional monomers share two oxygen atoms with the terminal tungstate (tetrahedral), resulting in the coordination change to octahedral. Once the seeds have been formed by the surface sorption, polymerization is driven by the addition of monomers. This model allows continued attachment from solution, and is therefore consistent with the isotherm results. With the present information, we cannot determine whether either of these possible mechanisms of tungstate polymerization is relevant in our experiments. Further studies using complementary approaches are needed to understand these mechanisms better.

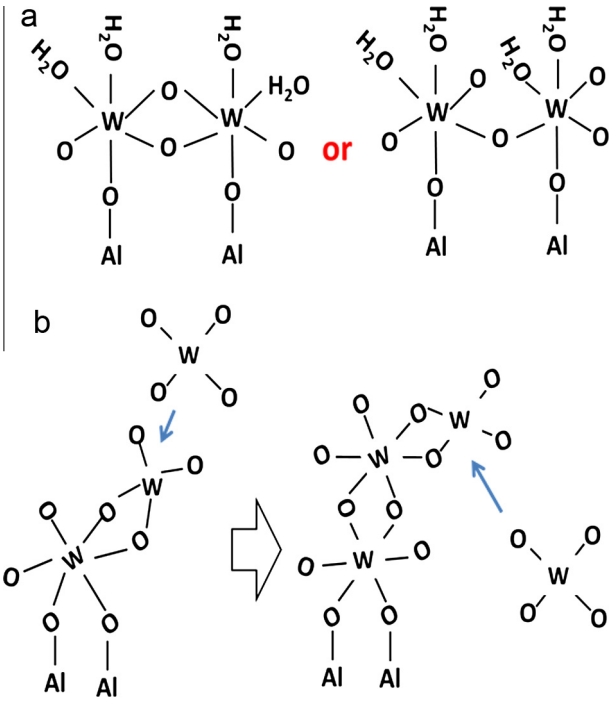

Fig. 9. Possible models for tungstate polymerization on the boehmite surface. The polymerization of neighboring tungstate surface complexes is shown in (a). The open chain polymerization mechanism is depicted in (b).

4.6. Possible environmental implications of tungstate polymerization

Strigul reported that speciation of tungstate is likely to be important for controlling its mobility, toxicity, and bioavailability in aquatic systems [1]. Our present findings demonstrate that tungstate forms stable polymeric surface complexes when sorbed on boehmite over a range of pH conditions. Hence the mobility of dissolved tungstate may be effectively limited by sorption on surfaces of (hydr)oxides, such as boehmite. However, we still lack an understanding of the toxicity and bioavailability of polytungstates bound on the surface of fine mineral particles in the environment. Evaluation of the toxicity of polytungstates sorbed on other mineral surfaces will be important for a complete understanding of the detailed environmental behavior of tungstate.

5. Conclusions

In this study, we examined the systematics and molecular-scale mechanisms of tungstate sorption onto boehmite over a range of pH values and tungstate concentrations. Batch uptake results reveal sorption behavior that is expected for anions, with tungstate binding strongly and irreversibly at low pH and less strongly with increasing pH. XAS analysis confirms the presence of polytungstate complexes on the surface over the pH range 4–8, although the exact tungstate species cannot be determined. Polymerization of tungstate appears to be favored during sorption onto boehmite. At pH 8, where monotungstate is the dominant solution species,

polymerization is accompanied by a change in coordination from tetrahedral (in solution) to octahedral in the surface complex. The results suggest that sorption onto boehmite is an effective means for environmental remediation of dissolved tungstate. The role of the mineral surface in favoring polymerization of tungstate remains unclear, and further studies should be undertaken using different sorbent phases. The results of this study are relevant for understanding tungstate mobility and bioavailability, which are strongly influenced by its sorption behavior, and should be accounted for in models concerned with the solubility, mobility, and accumulation of tungsten species in natural environments.

Acknowledgements

We thank Robert Rieger of the Stony Brook University Proteomics Center for assisting with ESI–MS data collection. The boehmite used in this study was provided by Dr. William Casey (UC Davis). This research was supported by the National Science Foundation, Grant CHE0714183. We also thank the beamline scientists at X11A, NSLS, and 12BM and 20BM, APS for their assistance with XAS measurements. Use of the National Synchrotron Light Source, Brookhaven National Laboratory, was supported by the U.S. Department of Energy, Office of Science, Office of Basic Energy Sciences, under Contract No. DE-AC02-98CH10886. Use of the Advanced Photon Source, an Office of Science User Facility operated for the U.S. Department of Energy (DOE) Office of Science by Argonne National Laboratory, was supported by the U.S. DOE under Contract No. DE-AC02-06CH11357. Comments from two anonymous reviewers improved the manuscript.

Appendix A. Supplementary material

Supplementary data associated with this article can be found, in the online version, at http://dx.doi.org/10.1016/j.jcis.2015.09.011.

References

[1] N. Strigul, Does speciation matter for tungsten ecotoxicology?, Ecotoxicol Environ. Safety 73 (6) (2010) 1099–1113.
[2] J.L. Clausen, N. Korte, Environmental fate of tungsten from military use, Sci. Total Environ. 407 (8) (2009) 2887–2893.
[3] A.J. Bednar, W.T. Jones, R.E. Boyd, D.B. Ringelberg, S.L. Larson, Geochemical parameters influencing tungsten mobility in soils, J. Environ. Qual. 37 (1) (2008) 229–233.
[4] B.J. Smith, V.A. Patrick, Quantitative determination of sodium metatungstate speciation by W-183 NMR spectroscopy, Aust. J. Chem. 53 (11–12) (2000) 965–970.
[5] J.J. Hastings, O.W. Howarth, A ^{183}W, ^{1}H and ^{17}O nuclear-magnetic-resonance study of aqueous isopolytungstates, J. Chem. Soc. Dalton Trans. 2 (1992) 209–215.
[6] J.J. Cruywagen, I.F.J. van der Merwe, Tungsten(VI) equilibria: a potentiometric and calorimetric investigation, J. Chem. Soc. Dalton Trans. 7 (1987) 1701–1705.
[7] D. Dermatas, W. Braida, C. Christodoulatos, N. Strigul, N. Panikov, M. Los, S. Larson, Solubility, sorption, and soil respiration effects of tungsten and tungsten alloys, Environ. Forensics 5 (1) (2004) 5–13.
[8] N. Strigul, A. Koutsospyros, P. Arienti, C. Christodoulatos, D. Dermatas, W. Braida, Effects of tungsten on environmental systems, Chemosphere 61 (2) (2005) 248–258.
[9] D.B. Ringelberg, C.M. Reynolds, L.E. Winfield, L.S. Inouye, D.R. Johnson, A.J. Bednar, Tungsten effects on microbial community structure and activity in a soil, J. Environ. Qual. 38 (1) (2009) 103–110.
[10] N. Strigul, A. Koutsospyros, C. Christodoulatos, Tungsten speciation and toxicity: acute toxicity of mono- and poly-tungstates to fish, Ecotoxicol. Environ. Safety 73 (2) (2010) 164–171.
[11] J.J. Cruywagen, Protonation, oligomerization, and condensation reactions of vanadate(V), molybdate(VI), and tungstate(VI), Adv. Inorg. Chem. 49 (2000) 127–182.
[12] J. Fierro, Metal Oxides: Chemistry and Applications, vol. 108, CRC Press, 2006.
[13] D.K. Walanda, R.C. Burns, G.A. Lawrance, E.I. von Nagy-Felsobuki, Electrospray mass spectrometry of aqueous solutions of isopolyoxotungstates, J. Cluster Sci. 11 (1) (2000) 5–28.
[14] J. Aveston, Hydrolysis of tungsten(VI): ultracentrifugation acidity measurements, and Raman spectra of polytungstates, Inorg. Chem. 3 (7) (1964) 981–986.
[15] J. Hernandez, Synthese de nanoparticules d'oxydes de fer et d'aluminium pour l'etude de l'adsorption d'entites inorganiques polycondensees, These de Doctorat de l'Universite Pierre et Marie Curie, Paris, 1998.
[16] N. Xu, C. Christodoulatos, W. Braida, Modeling the competitive effect of phosphate, sulfate, silicate, and tungstate anions on the adsorption of molybdate onto goethite, Chemosphere 64 (8) (2006) 1325–1333.
[17] J.P. Gustafsson, Modelling molybdate and tungstate adsorption to ferrihydrite, Chem. Geol. 200 (1–2) (2003) 105–115.
[18] S. Sugiyama, Y. Kanda, H. Ishizuka, K. Sotowa, Removal and regeneration of aqueous divalent cations by boehmite, J. Colloid Interface Sci. 320 (2) (2008) 535–539.
[19] W. Li, J. Feng, K.D. Kwon, J.D. Kubicki, B.L. Phillips, Surface speciation of phosphate on boehmite (γ-AlOOH) determined from NMR spectroscopy, Langmuir 26 (7) (2010) 4753–4761.
[20] T.J. Strathmann, S.C.B. Myneni, Effect of soil fulvic acid on nickel(II) sorption and bonding at the aqueous-boehmite (γ-AlOOH) interface, Environ. Sci. Technol. 39 (11) (2005) 4027–4034.
[21] F. Granados-Correa, J. Jimenez-Becerril, Chromium (VI) adsorption on boehmite, J. Hazard. Mater. 162 (2–3) (2009) 1178–1184.
[22] J. Nordin, P. Persson, E. Laiti, S. Sjoberg, Adsorption of o-phthalate at the water-boehmite (γ-AlOOH) interface: evidence for two coordination modes, Langmuir 13 (15) (1997) 4085–4093.
[23] C. Su, D.L. Suarez, In situ infrared speciation of adsorbed carbonate on aluminum and iron oxides, Clays Clay Miner. 45 (6) (1997) 814–825.
[24] M. Newville, IFEFFIT: interactive XAFS analysis and FEFF fitting, J. Synchrotron Rad. 8 (2001) 322–324.
[25] T. Ressler, WinXAS: a new software package not only for the analysis of energy-dispersive XAS data, J. Phys. IV 7 (C2) (1997) 269–270.
[26] S.I. Zabinsky, J.J. Rehr, A. Ankudinov, R.C. Albers, M.J. Eller, Multiple-scattering calculations of X-ray absorption spectra, Phys. Rev. B 52 (4) (1995) 2995–3009.
[27] W. Li, X.H. Feng, Y.P. Yan, D.L. Sparks, B.L. Phillips, Solid-state NMR spectroscopic study of phosphate sorption mechanisms on aluminum (hydr) oxides, Environ. Sci. Technol. 47 (15) (2013) 8308–8315.
[28] A. van Geen, A.P. Robertson, J.O. Leckie, Complexation of carbonate species at the goethite surface: implications for adsorption of metal ions in natural waters, Geochim. Cosmochim. Acta 58 (9) (1994) 2073–2086.
[29] M. Villalobos, J.O. Leckie, Carbonate adsorption on goethite under closed and open CO_2 conditions, Geochim. Cosmochim. Acta 64 (22) (2000) 3787–3802.
[30] S. Yamazoe, Y. Hitomi, T. Shishido, T. Tanaka, XAFS study of tungsten L_1- and L_3-edges: structural analysis of WO_3 species loaded on TiO_2 as a catalyst for photo-oxidation of NH_3, J. Phys. Chem. C 112 (17) (2008) 6869–6879.
[31] A. Kuzmin, J. Purans, Local atomic and electronic structure of tungsten ions in AWO_4 crystals of scheelite and wolframite types, Rad. Meas. 33 (5) (2001) 583–586.
[32] A. Kuzmin, J. Purans, M. Benfatto, C.R. Natoli, X-ray-absorption study of rhenium L_3 and L_1 edges in ReO_3: multiple-scattering approach, Phys. Rev. B 47 (5) (1993) 2480–2486.
[33] T. Kashiwabara, Y. Takahashi, M.A. Marcus, T. Uruga, H. Tanida, Y. Terada, A. Usui, Tungsten species in natural ferromanganese oxides related to its different behavior from molybdenum in oxic ocean, Geochim. Cosmochim. Acta 106 (2013) 364–378.
[34] Y. Tang, R.J. Reeder, Enhanced uranium sorption on aluminum oxide pretreated with arsenate. Part I: Batch uptake behavior, Environ. Sci. Technol. 43 (12) (2009) 4446–4451.
[35] Y. Tang, J. McDonald, R.J. Reeder, Enhanced uranium sorption on aluminum oxide pretreated with arsenate. Part II: Spectroscopic studies, Environ. Sci. Technol. 43 (12) (2009) 4452–4458.
[36] J.L. Clausen, B.C. Bostick, A. Bednar, J. Sun, J.D. Landis, Tungsten Speciation in Firing Range Soils, U.S. Army Corps of Engineers, Engineer Research and Development Center TR-11-1, 2011.
[37] Y. Arai, X-ray absorption spectroscopic investigation of molybdenum multinuclear sorption mechanism at the goethite–water interface, Environ. Sci. Technol. 44 (22) (2010) 8491–8496.
[38] L.E. Wasylenki, C.L. Weeks, J.R. Bargar, T.G. Spiro, J.R. Hein, A.D. Anbar, The molecular mechanism of Mo isotope fractionation during adsorption to birnessite, Geochim. Cosmochim. Acta 75 (17) (2011) 5019–5031.
[39] F. Hilbrig, H.E. Gobel, H. Knozinger, H. Schmelz, B. Lengeler, X-ray absorption spectroscopy study of the titania- and alumina-supported tungsten oxide system, J. Phys. Chem. 95 (18) (1991) 6973–6978.
[40] J.A. Horsley, I.E. Wachs, J.M. Brown, G.H. Via, F.D. Hardcastle, Structure of surface tungsten oxide species in the WO_3/Al_2O_3 supported oxide system from X-ray absorption near-edge spectroscopy and Raman spectroscopy, J. Phys. Chem. 91 (15) (1987) 4014–4020.
[41] C.T.J. Mensch, J.A.R. Vanveen, B. Vanwingerden, M.P. Vandijk, Extended X-ray absorption fine-structure study of Mo/Al_2O_3 samples prepared by equilibrium adsorption of ammonium heptamolybdate, J. Phys. Chem. 92 (17) (1988) 4961–4964.
[42] S.R. Bare, G.E. Mitchell, J.J. Maj, G.E. Vrieland, J.L. Gland, Local site symmetry of dispersed molybdenum oxide catalysts: XANES at the Mo $L_{2,3}$-edges, J. Phys. Chem. 97 (22) (1993) 6048–6053.
[43] H. Aritani, T. Tanaka, T. Funabiki, S. Yoshida, K. Eda, N. Sotani, M. Kudo, S. Hasegawa, Study of the local structure of molybdenum–magnesium binary oxides by means of Mo L_3-edge XANES and UV-vis spectroscopy, J. Phys. Chem. 100 (50) (1996) 19495–19501.

[44] S. Takenaka, T. Tanaka, T. Funabiki, S. Yoshida, Structures of molybdenum species in silica-supported molybdenum oxide and alkali-ion-modified silica-supported molybdenum oxide, J. Phys. Chem. B 102 (16) (1998) 2960–2969.
[45] R. Radhakrishnan, C. Reed, S.T. Oyama, M. Seman, J.N. Kondo, K. Domen, Y. Ohminami, K. Asakura, Variability in the structure of supported MoO_3 catalysts: studies using Raman and X-ray absorption spectroscopy with ab initio calculations, J. Phys. Chem. B 105 (36) (2001) 8519–8530.
[46] E.J. Lede, F.G. Requejo, B. Pawelec, J.L.G. Fierro, XANES Mo L-edges and XPS study of Mo loaded in HY zeolite, J. Phys. Chem. B 106 (32) (2002) 7824–7831.
[47] T. Kashiwabara, Y. Takahashi, M. Tanimizu, A. Usui, Molecular-scale mechanisms of distribution and isotopic fractionation of molybdenum between seawater and ferromanganese oxides, Geochim. Cosmochim. Acta 75 (19) (2011) 5762–5784.